Journal of ELECTRONIC MATERIALS, Vol. 44, No. 8, 2015
DOI: 10.1007/s11664-015-3763-z

Characterization, Luminescence, and Defect Centers of a Ce^{3+}-Doped $Li_2Si_2O_5$ Phosphor Prepared by a Solution Combustion Reaction

VIJAY SINGH,[1,5] S. WATANABE,[2] T.K. GUNDU RAO,[2] R. SENTHIL KUMARAN,[3] HUI GAO,[1] JINGLIN LI,[1] and HO-YOUNG KWAK[4]

1.—Department of Chemical Engineering, Konkuk University, Seoul 143-701, Republic of Korea. 2.—Institute of Physics, University of Sao Paulo, Sao Paulo, SP 05508-090, Brazil. 3.—Department of Biological Engineering, Konkuk University, Seoul 143-701, Republic of Korea. 4.—Mechanical Engineering Department, Chung-Ang University, Seoul 156-756, Republic of Korea. 5.—e-mail: vijayjiin2006@yahoo.com

$Li_2Si_2O_5$ doped with Ce was synthesized by solution combustion. The phosphor was characterized by powder x-ray diffraction (XRD), Fourier-transform infrared (FTIR) spectroscopy, and scanning electron microscopy (SEM). Photoluminescence was investigated by excitation with UV radiation at 244 nm. An emission peak of the Ce^{3+} ion was observed at 400 nm. Gamma irradiated phosphor exhibits six thermoluminescence (TL) peaks at 110°C, 160°C, 190°C, 250°C, 320°C, and 370°C. Electron spin resonance (ESR) spectroscopy was used to study the defect centers induced in the phosphor by gamma irradiation and to identify the centers responsible for the TL process. The room-temperature ESR spectrum of the irradiated phosphor seemed to be a superposition of at least four distinct centers. One of the centers (center I) with principal g values $g_{||} = 2.0307$ and $g_{\perp} = 2.0040$ was identified as an O_2^- ion. Center II, with an isotropic g factor 2.0070, was identified as an F^+-type center (singly ionized oxygen vacancy); this center correlates with the main low-temperature TL peak at 110°C. Center III was identified as a Ti^{3+} center and center IV, with a hyperfine interaction with a ^{29}Si nucleus, as an intrinsic O^--type center with a neighboring silicon ion. A Ti^{4+}ion, the precursor of the Ti^{3+} center, acts as a recombination center for the 110°C TL peak whereas a Ti^{3+} center relates to the main 250°C TL peak and is also the likely recombination center for this peak. An O^- ion is associated with the 110°C TL peak as a possible recombination center. An additional defect center (V) was observed during thermal annealing experiments. This center (identified as an F^+ center) seems to originate from an F center (oxygen vacancy with two electrons) and is not related to the any of the observed TL peaks.

Key words: Photoluminescence, doping, phosphors, ESR, combustion, defect centers

INTRODUCTION

Alkali metal silicate oxides have interesting physicochemical properties. Among the alkali metal silicate oxides, lithium silicate oxides have a wide range of applications in solid-state electrolyte lithium batteries, in absorption of carbon dioxide, as tritium breeding materials, as fast ion conductors, and in glass manufacture.[1–5] The crystal structure of alkali metal silicates has been investigated by use of IR spectroscopy, ^{29}Si NMR spectroscopy, and

(Received October 26, 2014; accepted March 24, 2015; published online April 10, 2015)

x-ray techniques.[6–8] Lithium orthosilicate (Li_4SiO_4) is a promising breeder material for fusion reactors.[9] The phase-separation behavior of lithium tetrasilicate ($Li_2Si_4O_9$) glass has been studied.[10–12] Morimoto investigated the effect of K_2O on crystallization of Li_2SiO_3 glass,[13] and the luminescence behavior of Li_2SiO_3 doped with Eu^{3+}, Tb^{3+}, and Ce^{3+} has also been studied.[14] The alkali metal silicate oxide of interest in this study is Ce-doped lithium disilicate ($Li_2Si_2O_5$). The first glass ceramic developed by Stookey was $Li_2Si_2O_5$.[15] The electronic structure of lithium disilicate ($Li_2Si_2O_5$) has been reported elsewhere.[16] $Li_2Si_2O_5$ has been investigated in detail, because of its high crystallinity and mechanical properties, and has a wide range of practical applications, especially for dental restorations.[17–19] A computational study of the structural, elastic, and electronic properties of $Li_2Si_2O_5$ glass ceramic was performed by Biskri et al.[20] The effect of manganese on the structure, crystallization, and sintering of nonstoichiometric $Li_2Si_2O_5$ glasses was investigated by Gaddam et al.[21] Paszkowicz et al.[22] have reported an x-ray diffraction and absorption study of crystalline vanadium-doped $Li_2Si_2O_5$. The physical properties of $Li_2Si_2O_5$ glasses doped with different amounts of V_2O_5 have been investigated before and after irradiation with gamma-rays.[23] The crystal growth behavior of CuO-doped $Li_2Si_2O_5$ glasses subjected to continuous-wave irradiation has been examined.[24] Zheng et al.[25] have investigated the effects of P_2O_5 content and heat treatment on the species present in the crystalline phase, and the microstructure of $Li_2Si_2O_5$ glass ceramics. The microstructure, and the mechanical, electron paramagnetic resonance, and optical properties of lithium disilicate glasses and glass ceramics doped with Mn^{2+} ions have been reported by Molla et al.[26]

A wealth of information about the luminescence properties of a variety of cerium-doped systems is available in the literature; as far as we are aware, however, there are no reports of studies of defects in cerium-doped $Li_2Si_2O_5$. There is also a shortage of information about the luminescence properties of $Li_2Si_2O_5$ phosphor, especially when doped with Ce^{3+} ions. It is well known that phosphor coatings in devices must be continuously exposed to ionizing radiation to furnish to visible light output. In this situation, formation of defect centers can be expected. Also, irradiation may change the charge states of defects and impurities in the lattice.[27] Some of the optical properties of the phosphor may be affected by these effects. In this context, we have studied the defect centers formed in Ce-doped $Li_2Si_2O_5$ phosphor by use of electron spin resonance spectroscopy. Efficient thermoluminescence (TL) was observed for several materials when suitable dopants, particularly rare earths, were present in the lattice.[28–30] The defect centers created by ionizing radiation, for example alpha, beta, and gamma radiation, are responsible for thermoluminescence of the solids. Identification and characterization of the defect centers are essential, because defects can have substantial effects on the physical and chemical properties of the solids. In previous studies we successfully synthesized rare-earth-doped aluminate and sulfide phosphors and investigated the effects of the defects formed by gamma irradiation and the effects of dopants on thermally stimulated luminescence.[28–32] Numerous ESR and TL studies have shown that defect centers affect the TL of solids. In recent years, several researchers have combined ESR, TL, and photoluminescence data to identify different defect and luminescence centers in several phosphors, and to obtain information about their decay.[28–36] Although the crystallization behavior of $Li_2Si_2O_5$ has been reported, there are few reports on that of $Li_2Si_2O_5$ doped with rare-earth ions, and detailed studies on combustion-synthesized Ce-doped $Li_2Si_2O_5$ have not been reported in the literature. In this study, Ce-doped $Li_2Si_2O_5$ phosphor was prepared by combustion synthesis and radiation-induced defects were investigated by study of thermoluminescence and by electron spin resonance spectroscopy.

EXPERIMENTAL

Synthesis

Trivalent cerium-doped $Li_2Si_2O_5$ of composition $Li_2Si_2O_5$:$Ce_{(0.01)}$ was prepared by combustion of $LiNO_3$, SiO_2, and glycine ($C_2H_5NO_2$) as precursor materials. In a typical synthesis, 2.0 g $LiNO_3$, 1.7432 g SiO_2, 0.0629 g $Ce(NO_3)_3{\cdot}6H_2O$, and 6.0687 g $C_2H_5NO_2$ were dissolved in a minimum quantity of deionized water in a 300-mL glass beaker. The resulting solution was reacted at 90°C for 20 min to obtain a homogenous solution. The solution was then placed in a muffle furnace preheated to 500°C. After the reaction, materials were crushed with a mortar and pestle and placed in 50-mL alumina crucibles to be heat-treated at 950°C for 5 h. The resulting powder was used for further characterization.

Characterization

X-ray diffraction data in the 2θ range 10–80° were recorded on an X'Pert Pro diffractometer (Panalytical) with $CuK\alpha_1$ radiation. Morphology was determined by use of a scanning electron microscope (SEM; Hitachi, Japan, S-3200 N). FTIR spectra in the range 4000–400 cm^{-1} were acquired by use of a Perkin–Elmer RX1 instrument. Photoluminescence measurement of excitation and emission were recorded by use of a Shimadzu RFPC5301 spectrofluorophotometer. Electron spin resonance experiments were performed with a Bruker EMX ESR spectrometer operating at the X-band frequency with 100 kHz modulation frequency. The g factors of signals were determined by use of a reference sample of diphenylpicrylhydrazyl (DPPH). The temperature dependence of the ESR spectra

was studied by use of the Bruker BVT 2000 variable-temperature accessory.

RESULTS AND DISCUSSION

X-Ray Diffraction

Figure 1 shows the x-ray diffraction pattern of $Li_2Si_2O_5$:Ce phosphor. The pattern is indicative of the monoclinic structure of $Li_2Si_2O_5$, which is consistent with the standard JCPDS powder diffraction data file, no. 72-0102. In addition, all the major diffraction peaks were observed, which indicates that the $Li_2Si_2O_5$ was successfully crystallized. However, there are additional secondary phases, marked with asterisks, because of the presence of unreacted precursors. This confirms reports that it is not easy to prepare a single-phase monoclinic structure.[37–39]

Scanning Electron Microscopy

Figure 2a, b, and c show low and high-magnification SEM images of $Li_2Si_2O_5$:Ce powder phosphor. A magnified region of Fig. 2a (region (a)) is shown in Fig. 2b. Similarly a magnified region of Fig. 2b (region (b)) is shown in Fig. 2c. Figure 2a and b show that the particles are non-uniform and irregular in shape and that the larger particles were formed by agglomeration and adhesion of smaller particles. The pores, voids, and cracks are formed because a large amount of gaseous matter escaped with high exothermicity. The higher-magnification images (Fig. 2b and c) show that the particles obtained from the combustion synthesis are normally interconnected. Because of the agglomerated nature of the particles, it was not possible to estimate accurate particle sizes from the SEM images.

FTIR

Fourier-transform infrared spectroscopy (FTIR) was used to obtain additional structural information. The FTIR transmittance spectrum of the phosphor in the wavenumber range 400–4000 cm^{-1} is shown in Fig. 3. The broad peak centered at 3442 cm^{-1} corresponds to O–H symmetric stretching of the surface hydroxyl group. In accordance with previous work,[7,22,26] the peaks observed between 400 cm^{-1} and 600 cm^{-1} can be ascribed to Si–O–Si and O–Si–O bending vibrations. The peaks observed between 700 cm^{-1} and 1200 cm^{-1} can be ascribed to Si–O–Si symmetric stretching and Si–O–Si asymmetric stretching. The peak corresponding to the stretching vibration is quite structured for this sample. Analysis of these results reveals they are in good agreement with previously reported results.[7,22,26,40]

Photoluminescence

Room-temperature photoluminescence spectra of $Li_2Si_2O_5$:Ce phosphor are shown in Fig. 4. Figure 4a and b show, respectively, the excitation and emission spectra of the phosphor. The excitation spectrum monitored at 400 nm contains a UV band maximum at 244 nm. Alemi et al.[41] recorded the excitation spectrum of undoped Li_2SiO_3 and $Li_2Si_2O_5$ nanomaterials. A band was observed with maxima at 360 and 250 nm. Figure 4b shows the emission spectrum of the $Li_2Si_2O_5$:Ce. The emission spectrum contains several weak bands in the region 440–650 nm and prominent bands with maxima at 400 nm when the excitation wavelength is fixed at 244 nm. A prominent emission band has a hump centered at 410 nm. This broad emission in the range of 325–650 nm could be attributed to both Ce^{3+} ions and defects in the host matrix, and several bands in the emission spectrum indicate that more than one emission center is present in this phosphor. Alemi et al.[41] recorded the emission spectrum of undoped Li_2SiO_3 and $Li_2Si_2O_5$ nanomaterials and observed bands at 410.03 nm and 291.45 nm.

TL and ESR

The TL glow curve of $Li_2Si_2O_5$:Ce phosphor for a 10-Gy gamma dose is shown in Fig. 5. Five TL peaks are observed at 110°C, 160°C, 190°C, 250°C, 320°C, and 370°C. The main TL peaks occur at approximately 110°C and 250°C with smaller peaks at 160°C, 190°C, 320°C and 370°C. A heating rate of 5°C/s was used to record the glow curves.

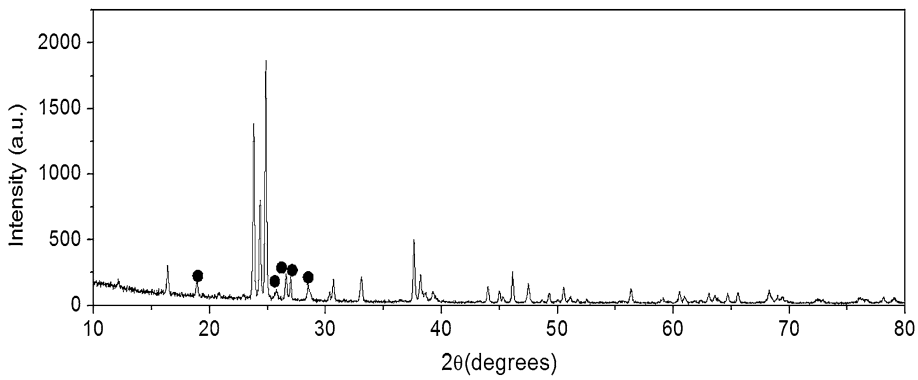

Fig. 1. Powder XRD pattern of $Li_2Si_2O_5$:Ce phosphor.

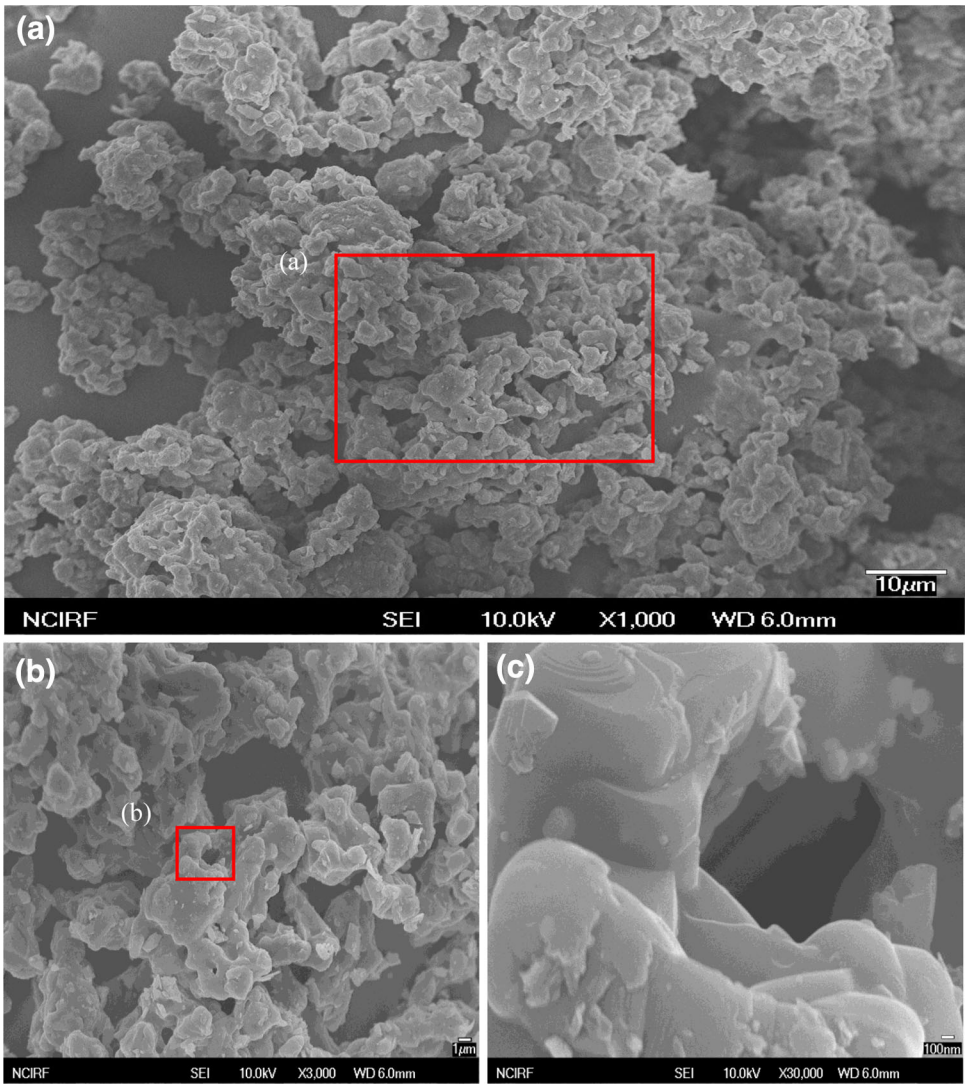

Fig. 2. SEM micrographs of $Li_2Si_2O_5$:Ce phosphor. A magnified region of Fig. 2a (red rectangle, region (a)) is shown in Fig. 2b. Similarly a magnified region of Fig. 2b (red square, region (b)) is shown in Fig. 2c.

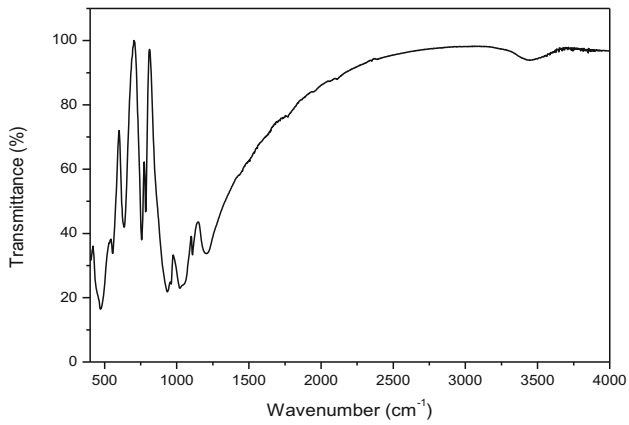

Fig. 3. Fourier-transform infrared spectrum of $Li_2Si_2O_5$:Ce phosphor.

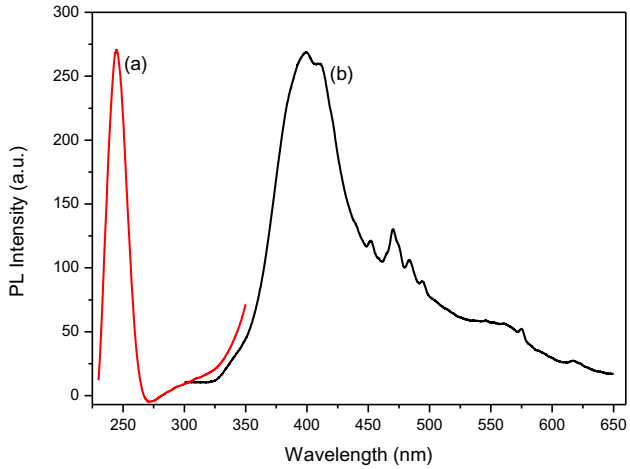

Fig. 4. Photoluminescence spectra. (a) Excitation spectrum of $Li_2Si_2O_5$:Ce phosphor (λ_{emi} = 400 nm). (b) Emission spectrum of $Li_2Si_2O_5$:Ce phosphor (λ_{exi} = 244 nm).

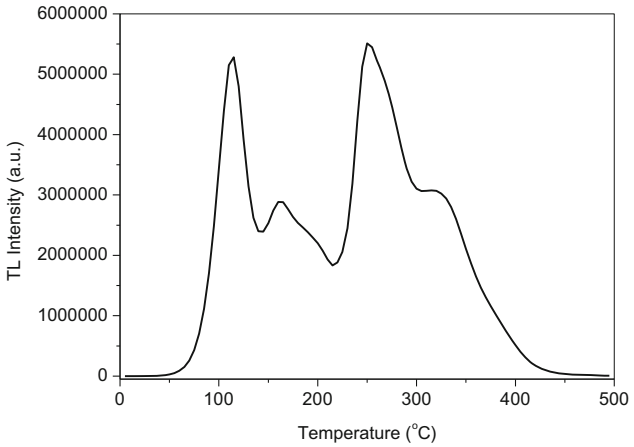

Fig. 5. TL glow curve of $Li_2Si_2O_5$:Ce phosphor (gamma dose:10 Gy).

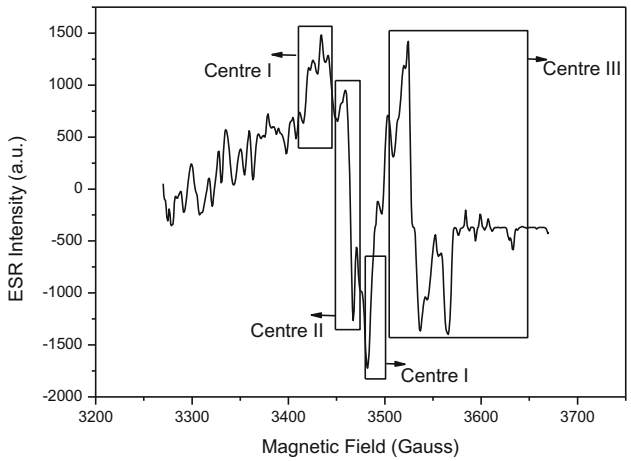

Fig. 6. Room temperature ESR spectrum of irradiated $Li_2Si_2O_5$:Ce phosphor (gamma dose: 10 kGy). The line labeled as I is because of an O_2- ion. The center II line is assigned to an F^+ center and center III is attributed to a Ti^{3+} center.

Lithium disilicate has the space group *Cc* but with strong orthorhombic pseudosymmetry *Ccc2*.[42] The unit cell contains four formula units and a total of 36 atoms. The structure consists of layers of SiO_4 tetrahedra networks with three bridging oxygen ions per tetrahedron. Lithium ions are also four-coordinated by oxygen and occupy regions between the silicon oxygen layers.

Mixed occupancy is expected at the Si site, with partial replacement by Li atoms. Therefore, on irradiation, several trapping sites for electron and holes are created because of antisite formation resulting from interchange of ions at tetrahedral and four-coordinated positions by monovalent and tetravalent ions. Further, changes in the defects and impurities charge states in the lattice are possible because of damage caused by irradiation.[43] These defects affect several of the optical and luminescent properties of the crystal.

Cation disorder and non-stoichiometry of $Li_2Si_2O_5$ can lead to a large number of lattice defects, which may serve as trapping centers. In this situation, irradiation can form F^+ centers by trapping electrons at oxygen vacancies. O^- ions can, however, be formed by hole trapping at silicon or lithium vacancies. Figure 6 shows the room temperature ESR spectrum of gamma-irradiated $Li_2Si_2O_5$:Ce phosphor (dose: 10 kGy). The spectrum seems to be a superposition of spectra from at least three defect centers; these centers are labeled in Fig. 6. This inference is based on thermal annealing experiments. A similar spectrum with more clarity and less noise was observed for irradiated undoped Li_2SiO_3; the corresponding ESR spectrum is shown in Fig. 7a. The spectrum from center I has no hyperfine structure and is characterized by an axially symmetric g tensor with principal values $g_{||} = 2.0415$ and $g_{\perp} = 2.0056$. Center I ESR lines are seen without overlap from the center II line after thermal annealing at 160°C; the corresponding spectrum is shown in Fig. 7b. In general, the centers most likely to be formed on gamma irradiation of a system such as $Li_2Si_2O_5$ are the V centers, F centers, and F^+ centers (an electron trapped in an anion vacancy). In a study on the binary oxide system Y_2O_3–CaO, Osada et al.[44] observed oxygen ions. ESR studies shows that these ions were characterized by an axial g tensor with principal values $g_{||} = 2.040$ and $g_{\perp} = 2.0030$. The oxygen ion has been ascribed to the superoxide ion O_2^- and is generated by adsorption of molecular oxygen by the binary oxide system. O_2^- ions with high g anisotropy have also been observed in several zeolites and metal oxides.[45–47] It should be noted that the $g_{||}$ value for the O_2^- ion was found to be highly matrix-dependent and ranged between 2.015 and 2.080. On the basis of these results, center I with relatively large anisotropy in g values in this system is tentatively assigned to an O_2^- ion. The stability of center I was measured by use of the pulsed thermal annealing method. The sample was heated to a given temperature, which was maintained for 3 min, then rapidly cooled to room temperature. The thermal annealing behavior of center I is shown in Fig. 8a. It is apparent that the center becomes unstable at approximately 150°C and decays in the broad temperature range 150°C–350°C. This decay appears to be related to the main TL peak at 250°C.

The ESR line labeled as II in Fig. 6 aries from a center characterized by a single ESR line with an isotropic g value equal to 2.0034 with 6 gauss linewidth. A probable center which can be trapped in this system is the F^+ center (an electron trapped in an anion vacancy). Such a center was first observed in neutron-irradiated LiF by Hutchison.[48] In neutron-irradiated LiF, a single line broad line (linewidth ~100 gauss) with a g factor equal to 2.008 was observed. A similar center is also produced in other systems, for example oxides and alkali metal halides, by x-ray or gamma irradiation. These centers are characterized by a small g shift, which may

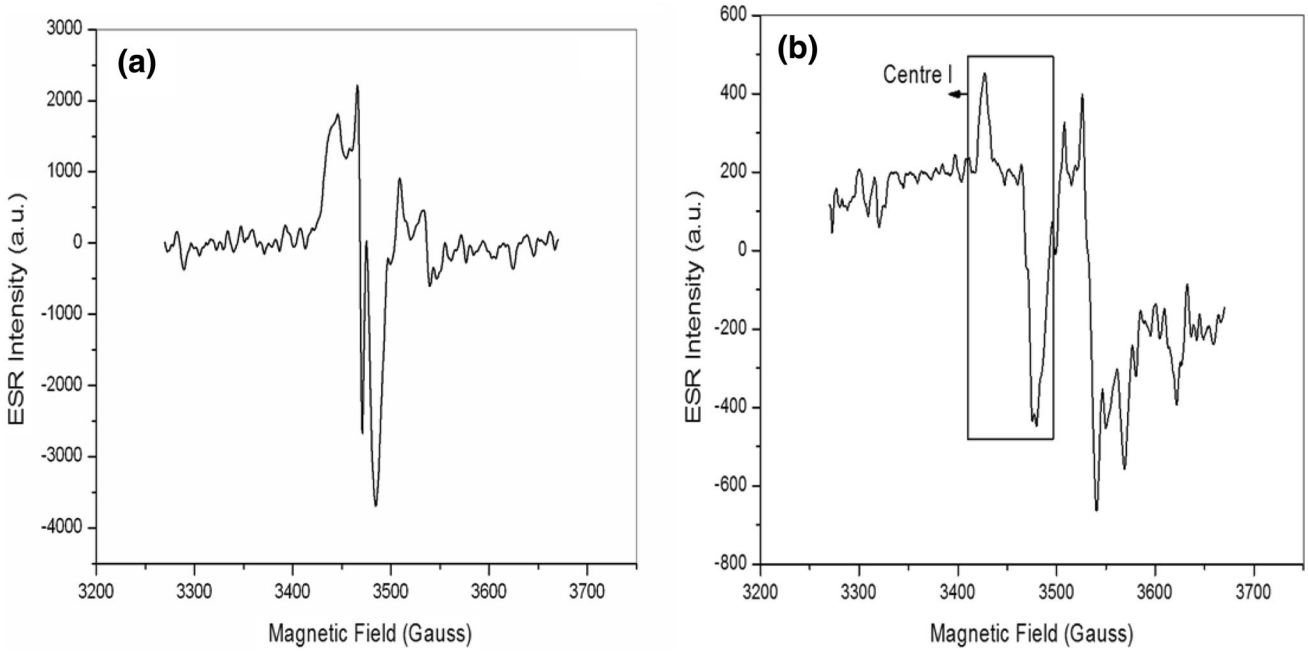

Fig. 7. (a) Room temperature ESR spectrum of irradiated Li_2SiO_3 (gamma dose: 10 kGy). ESR lines associated with centers I, II, and III in $Li_2Si_2O_5$:Ce phosphor are stronger and more clearly seen in this system. (b) ESR spectrum of $Li_2Si_2O_5$:Ce phosphor after thermal annealing at 160°C. Center I (O_2^- ion) lines are seen without overlap from center II lines.

be positive or negative, and a line width which depends on the host system.

An electron can be trapped in an anionic vacancy as a result of irradiation, and this is the basis for formation of F^+ centers. A major contribution to the linewidth is hyperfine interaction with nearest-neighbor (nn) cations. Defect center II formed in this system is characterized by a small g shift, and the linewidth is not large. On the basis of these observations, and consideration of the characteristic features of the defect centers likely to be formed in a system such as $Li_2Si_2O_5$:Ce, center II is tentatively identified as an F^+ center.

A pulsed thermal-annealing technique was used to measure the stability of center II. The thermal annealing behavior of center II is shown in Fig. 8b. It is observed that the intensity of the ESR line associated with this center decreases in the temperature range 70–140°C. Center II seems to correlate with the low-temperature TL peak at 110°C.

The center associated with the ESR lines labeled as III in Fig. 6 is characterized by a rhombic g tensor with principal values $g_1 = 1.9836$, $g_2 = 1.9717$, and $g_3 = 1.9204$. In one of the earliest ESR studies of defects in quartz, Wright et al.[49] identified paramagnetic centers in rose quartz which arise from titanium ions present in silicon sites. Two titanium centers, called A.Ti–Li and A.Ti-H, formed by room temperature x-irradiation were observed with principal g values of $g_1 = 1.9788$, $g_2 = 1.9310$, and $g_3 = 1.9120$ and $g_1 = 1.9856$, $g_2 = 1.9310$, and $g_3 = 1.9151$, respectively. It was suggested that an electron, removed from such sources as aluminium–alkali metal sites, is trapped by the titanium central atom located within the quartet of neighboring oxygen atoms. An alkali metal or hydrogen ion acts as a charge compensator and interacts with two nearest members of the oxygen quartet and gives stability to the Ti center. The rose quartz crystals studied by Wright et al. do not give ESR signals in their virgin state and give stable Ti center signals only after x-irradiation at room temperature. Center III ESR signals observed in this study has similar g values, stability, and formation behavior (after room-temperature irradiation) as Ti^{3+} centers observed in rose quartz. On the basis of these observations, center III is tentatively assigned as a Ti^{3+} center.

The thermal annealing behavior of the Ti^{3+} center is shown in Fig. 8c. It was observed that the concentration of these centers increases in the temperature range 40–160°C. This increase would be possible if Ti^{4+} ions, the precursors of the Ti^{3+} centers, are converted to Ti^{3+} centers by capture of an electron. It was observed that center II decays in the temperature range 70–140°C. Taken together with the observations on Ti^{3+} centers, it is speculated that the electrons released by center II are combining with Ti^{4+} ions, leading to an increase in the concentration of Ti^{3+} centers. Consequently, Ti^{4+} ions act as the recombination centers for the 110°C TL peak. Starting from approximately 160°C, Ti centers begin to decay. Because decay of center III is observed in the temperature range 160–340°C,

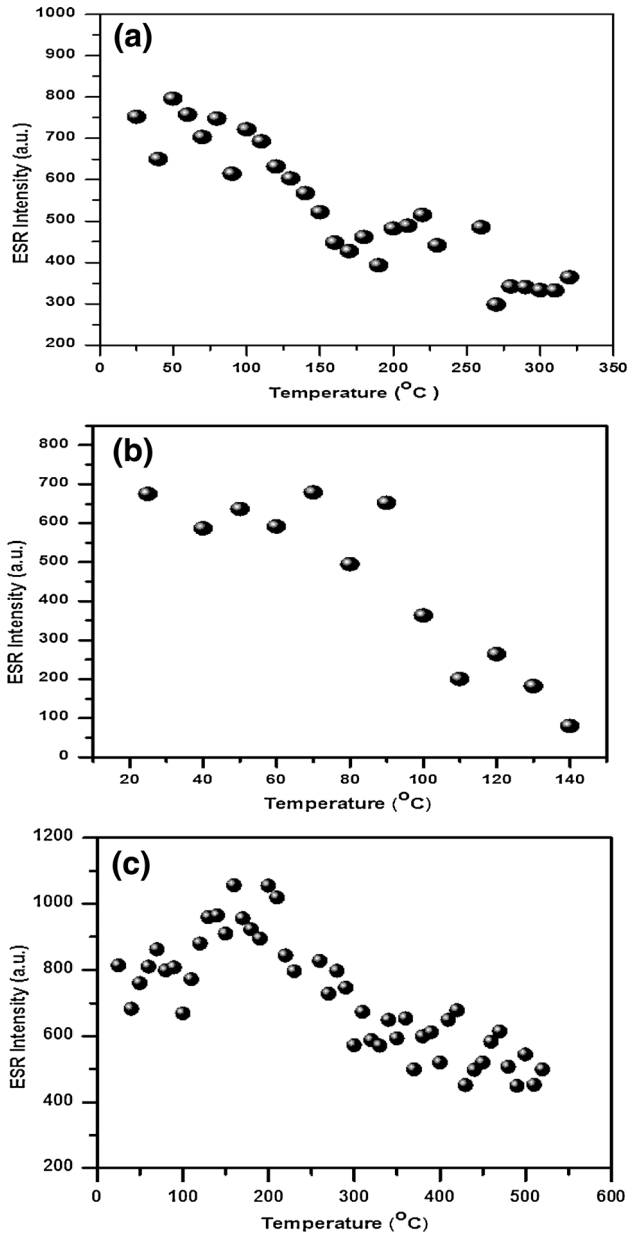

Fig. 8. (a) Thermal annealing behavior of center I in $Li_2Si_2O_5$:Ce phosphor. (b) Thermal annealing behavior of center II in $Li_2Si_2O_5$:Ce phosphor. (c) Thermal annealing behavior of center III in $Li_2Si_2O_5$:Ce phosphor.

center III may be related to the TL peak at 250°C and also seems to be the recombination center for this TL peak.

Apart from the ESR lines seen near the free-electron resonance, a two-line spectrum is observed with a large magnetic field scan extending from 2,500 to 4,500 gauss. The corresponding ESR spectrum is shown in Fig. 9a. The two lines seem to originate from the hyperfine interaction of the unpaired electron with a spin ½ nucleus. It is speculated that this interaction is because of a silicon atom (^{29}Si, I = 1/2, 4.68% natural abundant). The center associated with the two-line spectrum is labeled as center IV (Fig. 9a) and has a g value of 2.0496. The line separation is approximately 1169 gauss. It was mentioned above that cation disorder and non-stoichiometry of $Li_2Si_2O_5$ can give rise to O^- ions, which are formed by hole trapping by lithium or silicon vacancies. Hence, center IV is tentatively assigned to an O^- ion stabilized by a nearby cation vacancy (a hole trapped in a Li^+/Si^{4+} ion vacancy). Hyperfine interaction is sometimes observed for O^--type hole centers, because of adjacent transition metal ions. For example, in an earlier study on $LiNbO_3$, Miki et al.[50] observed hyperfine structure for the O^- hole center as a result of three neighboring ions. For Li_3VO_4, however, Murata et al.[51] observed that the O^- ions interact with one vanadium ion. In Li_3VO_4, each oxygen has one nearest neighbor vanadium ion and, consequently, hyperfine interaction with the nearest-neighbor vanadium ion is observed for the O^- ion formed in this system. Similarly, the hole trapped by oxygen of the SiO_4 tetrahedron in $Li_2Si_2O_5$ could be interacting with a nearest-neighbor silicon, giving rise to the two line spectrum observed. The thermal annealing behavior of center IV is shown in Fig. 9b. It is observed that the center becomes unstable at approximately 90°C and decays in the temperature range 90–140°C. Hence, the O^- ion could be associated with the main 110°C TL peak, and it is also speculated that the electrons released from F^+ centers (center II) are combining with the holes trapped by the O^- ion, rendering this center a recombination center for the 110°C TL peak.

During thermal annealing experiments a new ESR line was observed at high temperatures. The ESR spectrum after thermal annealing at 400°C is shown in Fig. 10a. The intensity of the new line is small and the associated defect center has an isotropic g value of 2.0036 with a 6-gauss line width. This center (V) is tentatively assigned to an F^+ center, for the reasons already mentioned. It should be mentioned that the formation behavior of the E_1'center in SiO_2 is similar. After a detailed study of SiO_2, Jani et al.[52] proposed an oxygen vacancy containing two electrons as the precursor of the E_1'center. This oxygen vacancy is likely to release an electron during post-irradiation heating, resulting in the formation of an E_1'center. On the basis of these results for SiO_2, it seems that in $Li_2Si_2O_5$:Ce phosphor the process of formation of center III might be similar.

The $Li_2Si_2O_5$:Ce lattice can contain oxygen vacancies as a result of non-stoichiometry and also because of the presence of impurity ions. Irradiation at room temperature can convert these vacancies into F centers which contain two electrons. During heating, F centers release an electron which is manifested during thermal annealing experiments as the appearance of center V. The two F^+ centers observed in this study have isotropic g values. However, they have some differences. The processes of formation of the centers are different. Center II is

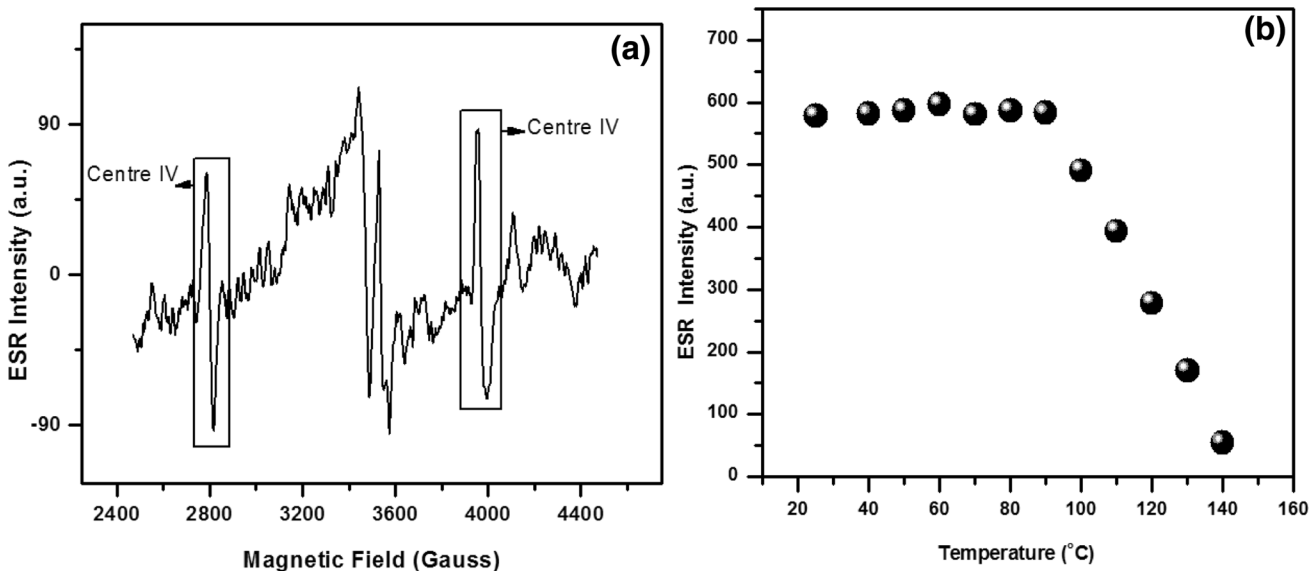

Fig. 9. (a) ESR lines from the O^- ion (center IV) in $Li_2Si_2O_5$:Ce phosphor, seen with a larger magnetic field scan. (b) Thermal annealing behavior of the O^- ion (center IV) in $Li_2Si_2O_5$:Ce^{3+} phosphor.

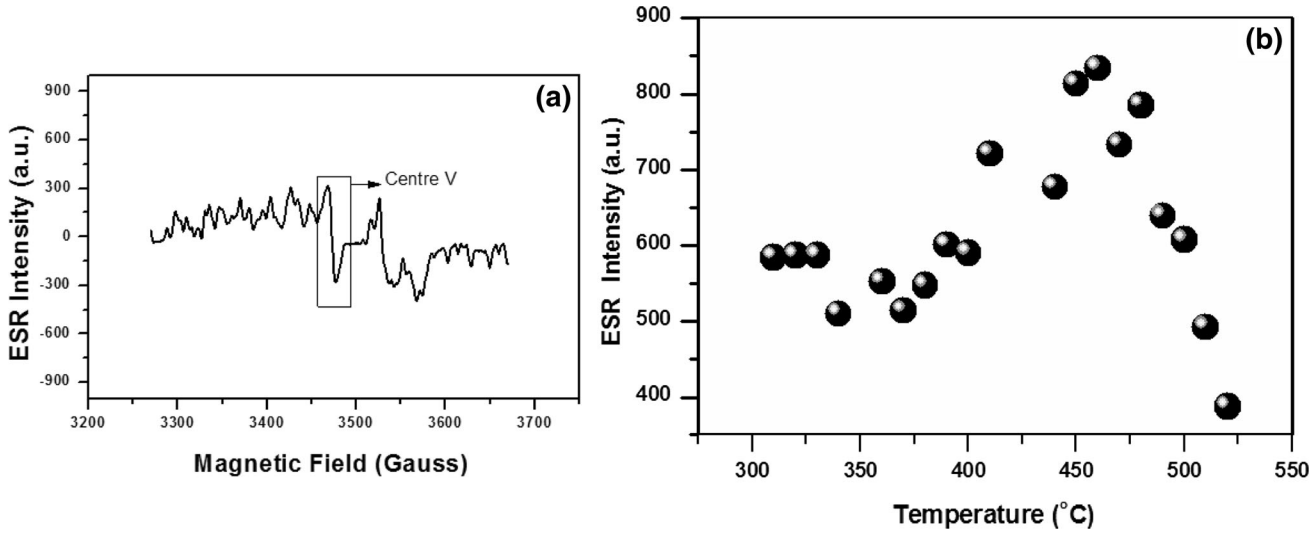

Fig. 10. (a) ESR spectrum of $Li_2Si_2O_5$:Ce phosphor after thermal anneal at 400°C. The line labeled "V" is ascribed to an F^+ center. (b) Thermal annealing behavior of center V in $Li_2Si_2O_5$:Ce^{3+} phosphor.

formed by capture of an electron by an anionic vacancy. Center V, on the other hand, is formed when sufficient thermal energy is given to an F center (an anion vacancy with two electrons) enabling it to release one of the electrons. This F^+ center, formed at high temperature, can release the remaining electron (unpaired electron) only at high temperature. Therefore, the thermal stability of center V is greater than that of center II.

The thermal annealing behavior of center V is shown in Fig. 10b. It is apparent that the center grows in the temperature range 370–460°C. Release of an electron by the F center with increasing temperature during thermal annealing is manifested as growth of center V in ESR experiments. The observed reduction in ESR signal intensity in the temperature range 460–520°C is because of the decay of the F^+ center. These results indicate that center V is not related to any of the observed TL glow peaks of this phosphor.

CONCLUSIONS

Ce-doped $Li_2Si_2O_5$ phosphor was synthesized by the combustion method. XRD indicated the monoclinic structure of the phosphor. The phosphor particles were irregular. FTIR results revealed symmetric Si–O–Si vibrations and O–Si–O asym-

metric vibrations. The emission spectrum on excitation at 244 nm contained a broad band with a maximum at 400 nm. The phosphor has six thermoluminescence peaks, with the dominant peaks at 110°C and 250°C. Four defect centers were identified for the room temperature-irradiated phosphor, and a fifth center was seen during thermal annealing experiments. These centers are tentatively assigned to an O_2^- ion, an O^- ion, a Ti^{3+} center, and two F^+ centers. The O_2^- ion and the Ti^{3+} center seem to be related to the main 250°C TL peak, with Ti^{3+} acting as a probable recombination center. Similarly, the O^- ion and the F^+ center (II) correlate with the other main 110°C TL peak, and the likely recombination center is the O^- ion. The second F^+ center (V) arising from a neutral F center (oxygen vacancy with two electrons) is not related to any of the observed TL peaks.

ACKNOWLEDGEMENTS

This paper was supported by the KU Research Professor Program of Knokuk University. T.K. Gundu Rao is grateful to CAPES, Brazil, for a research fellowship.

REFERENCES

1. M.P. Borom, A.M. Turkalo, and R.H. Doremus, *J. Am. Ceram. Soc.* 58, 385 (1975).
2. G.J. Gardopee, R.E. Newnham, and A.S. Bhalla, *Ferroelectrics* 33, 155 (1981).
3. K. Ben Saad, H. Hamzaoui, A. Labidi, and B. Bessaïs, *Appl. Surf. Sci*. 254, 3955 (2008).
4. J.R. Jacquin and M. Tomozawa, *J. Non-Cryst. Solids* 190, 233 (1995).
5. A. Nyten, A. Abouimrane, M. Armand, T. Gustafsson, and J.O. Thomas, *Electrochem. Commun*. 7, 156 (2005).
6. C. Bischoff, H. Eckert, E. Apel, V.M. Rheinberger, and W. Höland, *Phys. Chem. Chem. Phys.* 13, 4540 (2011).
7. T. Fuss, A. Mogus-Milankovic, C.S. Ray, C.E. Lesher, R. Youngman, and D.E. Day, *J. Non-Cryst. Solids* 352, 4101 (2006).
8. T. Fuss, C.S. Ray, C.E. Lesher, and D.E. Day, *J. Non-Cryst. Solids* 352, 2073 (2006).
9. E. Carella and T. Hernández, *Phys. B* 407, 4431 (2012).
10. Y. Moriya, D.H. Warrington, and R.W. Douglas, *Phys. Chem. Glasses* 8, 19 (1967).
11. S.S. Kim and T.H. Sanders Jr, *J. Am. Ceram. Soc.* 74, 1833 (1991).
12. S. Sen and F. Stebbines, *Phys. Rev. B* 50, 822 (1994).
13. S. Morimoto, *J. Ceram. Soc. Jpn.* 114, 195 (2006).
14. Y.P. Naik, M. Mohapatra, N.D. Dahale, T.K. Seshagiri, V. Natarajan, and S.V. Godbole, *J. Lumin.* 129, 1225 (2009).
15. S.D. Stookey, *Ind. Eng. Chem.* 45, 115 (1953).
16. J. Du and L.R. Corrales, *J. Phys. Chem.* 110, 22346 (2006).
17. W. Höland, V. Rheinberger, E. Apel, and C. van't Hoen, *J. Eur. Ceram. Soc*. 27, 1521 (2007).
18. Lithium silicate glass ceramic, US Patent 7452836 (2008).
19. W. Hölland, V. Rheinberger, E. Apel, C. Ritzberger, F. Rothbrust, H. Kappert, F. Krumeich, and R. Nesper, *J. Eur. Ceram. Soc.* 29, 1291 (2009).
20. Z.E. Biskri, H. Rached, M. Bouchear, and D. Rached, *J. Mech. Behav. Biomed. Mater*. 32, 345 (2014).
21. A. Gaddam, H.R. Fernandes, D.U. Tulyaganov, M.J. Pascual, and José M.F. Ferreira, *RSC Adv*. 26, 13581 (2014).
22. W. Paszkowicz, A. Wolska, M.T. Klepka, S. abd el All, and F.M. Ezz-Eldin, *Acta Phys. Pol., A* 117, 315 (2010).
23. S. Abd El All and F.M. Ezz-Eldin, *Nucl. Instrum. Methods B* 268, 49 (2010).
24. T. Honma, P.T. Nguyen, and T. Komatsu, *J. Ceram. Soc. Jpn.* 116, 1314 (2008).
25. X. Zheng, G. Wen, L. Song, and X.X. Huang, *Acta Mater.* 56, 549 (2008).
26. A.R. Molla, R.P.S. Chakradhar, C.R. Kesavulu, J.L. Rao, and S.K. Biswas, *J. Alloys Compd.* 512, 105 (2012).
27. G.P. Summers, G.S. White, K.H. Lee, and J.H. Crawford, *Phys. Rev. B* 21, 2578 (1980).
28. V. Singh, T.K. Gundu Rao, and D.-K. Kim, *Radiat. Meas.* 43, 1198 (2008).
29. V. Singh and T.K. Gundu Rao, *J. Solid State Chem*. 181, 1387 (2008).
30. V. Singh, T.K. Gundu Rao, and J.-J. Zhu, *J. Lumin.* 126, 1 (2007).
31. V. Singh, J.-J. Zhu, T.K. Gundu Rao, M. Tiwari, and P.H. Cheng, *Chin. Phys. Lett.* 22, 3182 (2005).
32. V. Singh, T.K. Gundu Rao, J.-J. Miao, and J.-J. Zhu, *Radiat. Eff. Defects Solids* 160, 265 (2005).
33. R. Hari Krishna, B.M. Nagabhushana, H. Nagabhushana, D.L. Monika, R. Sivaramakrishna, C. Shivakumara, R.P.S. Chakradhar, and T. Thomas, *J. Lumin*. 155, 125 (2014).
34. O. Annalakshmi, M.T. Jose, U. Madhusoodanan, J. Sridevi, B. Venkatraman, G. Amarendra, and A.B. Mandal, *Radiat. Eff. Defects Solids* 169, 636 (2014).
35. V. Singh, S. Borkotoky, A. Murali, J.L. Rao, T.K. Gundu Rao, and S.J. Dhoble, *Spectrochim. Acta A* 139, 1 (2015).
36. S. Watanabe, T.K. Gundu Rao, P.S. Page, and B.C. Bhatt. *J. Lumin.* 130, 2146 (2010).
37. T. Zhao, Y. Qin, P. Zhang, B. Wang, and J.-F. Yang, *Ceram. Int.* 40, 12449 (2014).
38. P. Zhang, X. Li, J. Yang, and X. Shaochun, *J. Non-Cryst. Solids* 402, 101 (2014).
39. P. Zhang, X. Li, J. Yang, and X. Shaochun, *J. Non-Cryst. Solids* 392–393, 26 (2014).
40. H.A. Elbatal, Z.S. Mandouh, H.A. Zayed, S.Y. Marzouk, G.M. Elkomy, and A. Hosny, *J. Non-Cryst. Solids* 358, 1806 (2012).
41. A. Alemi, S. Khademinia, S.W. Joo, M. Dolatyari, and A. Bakhtiari, *Int. Nano Lett.* 3, 14 (2013).
42. V.F. Liebau, *Acta Crystallogr.* 14, 389 (1961).
43. G.P. Summers, G.S. White, K.H. Lee, and J.H. Crawford, *Phys. Rev. B* 21, 2578 (1980).
44. Y. Osada, S. Koike, T. Fukushima, S. Ogasawara, T. Shikada, and T. Ikariya, *Appl. Catal.* 59, 59 (1990).
45. D.D. Eley and M.A. Zammitt, *J. Catal.* 21, 366 (1971).
46. K.M. Wong and J.H. Lunsford, *J. Phys. Chem.* 74, 1165 (1971).
47. J.H. Lunsford, *Catal. Rev*. 8, 135 (1973).
48. C.A. Hutchison, *Phys. Rev.* 75, 1769 (1949).
49. P.M. Wright, J.A. Weil, T. Buch, and J.H. Anderson, *Nature* 197, 246 (1963).
50. T. Miki, M.R. Hantehzadeh, and L.E. Halliburton, *J. Phys. Chem. Solids* 50, 1003 (1989).
51. T. Murata and T. Miki, *J. Appl. Phys.* 73, 1110 (1993).
52. M.G. Jani, R.B. Bossoli, and L.E. Halliburton, *Phys. Rev. B* 27, 2285 (1983).